

## **A Temperature-insensitive Bragg grating sensor - Using orthogonal polarisation modes for in-situ temperature compensation**

Richard M. Parker<sup>a,b,†</sup>, James C. Gates<sup>a</sup>, Martin C. Grossel<sup>b</sup>, Peter G. R. Smith<sup>a</sup>

<sup>a</sup>*Optoelectronics Research Centre, <sup>b</sup>School of Chemistry, University of Southampton, Southampton, United Kingdom, SO17 1BJ.*

*†corresponding author; rmp@orc.soton.ac.uk*

An exposed Bragg grating incorporated into a planar waveguide forms an optical device that acts as a refractive index sensor. The exposed evanescent field causes the Bragg peak to be sensitive to the refractive index of its surroundings and can be used to detect changes in this environment. The method reported is able to provide accurate temperature compensation by applying a scaling factor derived from measurement of the birefringence of the transverse electric (TE) and transverse magnetic (TM) modes of the Bragg reflection. For a fluid sensor, fluctuations in ambient temperature can be both accounted for and compensated to produce a temperature-insensitive sensor.

Keywords: Bragg grating, refractive index sensor, TE and TM modes, integrated optics.

## 1. Introduction

The field of integrated optics focuses on fabricating devices that integrate together multiple photonic functions [1]. The incorporation and miniaturisation of a range of functions within a single device offers smart sensors for chemical analysis and biomedical diagnostics.

While there are many competing approaches to sensors within integrated optics, including Surface Plasmon Resonance sensors [2] (SPR) and Mach Zehnder interferometers [3], there are several key advantages to using a Bragg grating system. The avoidance of heavy metals (such as gold) within the device reduces both the cost and the environmental impact of the sensor, while still retaining a functionalisable sensor surface [4]. The ease of measuring the single variable of the peak Bragg wavelength allows for straightforward interpretation of the sensing environment. Fibre-coupled, integrated Bragg grating sensors can be easily incorporated into distributed networks, with centralised interrogation by standard telecoms test and measurement equipment. This reduces the cost by allowing multiple sensors to be centrally interrogated by a single hub analysis station. Furthermore, the small size and integrated nature allows for the optical sensors to be deployed for a wide range of applications including use within flammable environments.

## 2. Background

Two dimensional planar waveguides can be written directly with a UV-laser into a photosensitised silica-on-silicon substrate to produce a wide range of integrated optical devices; from splitters and couplers to Mach Zehnder interferometers, without the need for photolithographic processing [5][6]. Furthermore, modulation of a pair of interfering beams allows Bragg gratings to be directly written simultaneously with the channel structure [7][8].

While these Bragg gratings are inherently sensitive to both temperature and strain, etching of the over-clad exposes the evanescent field of the fundamental mode to the ambient environment [9] (Figure 1(a)). Changes in this environment alter the effective refractive index ( $n_{\text{eff}}$ ) of the Bragg grating and can be monitored by the corresponding shift in peak Bragg wavelength ( $\lambda_B$ ). The sensitivity of the device to changes in refractive index is strongly dependent on the fraction of the evanescent field that penetrates into the analyte. A thin layer of a high index material, such as tantalum pentoxide over the etched region of the waveguide increases the sensitivity by pulling the guided mode up into the analyte (Figure 1(b))[3]. Sputtered deposition of tantalum pentoxide directly onto the sensor surface has been shown to increase the sensitivity to refractive index by up to an order of magnitude, without significant reduction in the reflected signal. The resultant sensitivity to bulk index change has been shown [10] to be in the order of  $10^{-6}$ .

The reflectance spectrum in the infrared region can be analysed via a fibre pigtail, allowing sub-picometre measurement of the peak wavelength of the Bragg grating. Changes in this Bragg wavelength can be used to provide information about the refractive index of the analyte. However, as the Bragg gratings intrinsically respond linearly with changes in temperature, ( $\sim 10 \text{ pm } ^\circ\text{C}^{-1}$ ), fluctuations in the ambient temperature is a significant problem. In practical sensor applications, thermal control of the ambient environment is not a viable solution, making temperature referencing a requirement.

The simplest solution to compensate for thermal drift, utilises an additional local Bragg grating of different Bragg wavelength written near to the etched region, a technique that works equally well within both fibre [11][12] and planar Bragg grating sensors [10]. If this is left un-etched, it remains insensitive to changes in analyte but is still sensitive to changes in temperature and strain. In this way, the Bragg response to changes in analyte refractive index within the etched

region can be separated from thermal effects by a simple first order approximation. However there are two disadvantages with this approach that become more apparent as the sensitivity of the system increases. Firstly, while the second reference Bragg grating is located close to the sensor grating, temperature gradients can exist between the two locations even on the same chip. In fast changing or microfluidic systems this lag in temperature referencing reduces the effectiveness of the thermal compensation. Secondly the mode structure and composition at the two Bragg gratings is markedly different; each grating will sense different thermo-optic properties. This results in a difference in  $dn_{\text{eff}}/dT$  between the reference and sensor gratings. While this temperature referencing technique is sufficient for simple systems; for the detection of the subtle changes in refractive index needed for practical chemical sensors, precise *in-situ* temperature referencing is required.

In this work we will show that by using orthogonal mode responses we can provide a more accurate compensation that addresses both of the limitations discussed above.

### 3. Experimental

A planar silica-on-silicon structure, where a germanium-doped core layer is confined between two silica cladding layers was fabricated by flame hydrolysis deposition. Into this structure, channel waveguides can be directly written with a UV-laser allowing simultaneous formation of both waveguides and Bragg gratings [7][8]. The UV-written waveguide dimensions were defined by the thickness of the planar core layer and the width of the UV beam. The Bragg gratings were 2 mm long with a period between 525 and 542 nm, satisfying the Bragg condition to reflect wavelengths between 1520 and 1570 nm.

The overclad was subsequently etched away with hydrofluoric acid to expose the evanescent field of the Bragg grating to the environment. By monitoring the etching process *in situ* through the Bragg response, the etch depth can be accurately and reproducibly controlled. Subsequent polishing allowed the surface to be restored to an optical quality. This was confirmed via atomic force microscopy (AFM), where the surface roughness after polishing was comparable to that of the un-etched surface. The reflectance spectrum of an infrared erbium fibre ASE source (1520 – 1570 nm) was analysed by an optical signal analyser (OSA) via a circulator connected to the device through a fibre pigtail. The central wavelength of the Bragg response was calculated from a Gaussian fit to the Bragg peak allowing for sub-picometre resolution.

All the modelling presented in this paper was performed using the commercial mode solver “Fimmwave”. The waveguide was modelled as a 0.005 step index increase for a square cross-section, within the 5.0  $\mu\text{m}$  core layer of index 1.4465. The index of the underclad was modelled to be 1.444, while the 72.5 nm thick tantalum pentoxide overlayer was found to be 2.05. The indices and thicknesses of the planar silica layers used in the modelling were determined using a Metricon prism coupler, while the tantalum pentoxide thickness was measured using a surface profiler. Although the real refractive index profile of both the planar core layer vertically and the channel laterally exhibit Gaussian like profiles, the precise refractive index profile of the waveguide is unknown. It has been previously shown that for weak index guidance a step refractive index profile for the modelled waveguide gives good agreement [13]. The model was corrected to compensate for the stress-induced birefringence inherent within the waveguide of the silica-on-silicon device, formed as a result of the flame hydrolysis deposition fabrication process.

The effective refractive index,  $n_{\text{eff}}$ , of the Bragg grating response represents the overall refractive index to which the guided mode is exposed to within the Bragg region. As such this is a combination of the refractive indices of the silica waveguide, the high index overlayer and any analyte present. In this work, this is presented as a shift relative to an initial

value rather than as an absolute index measurement. The shift in effective refractive index ( $\Delta n_{\text{eff}}$ ) is simply calculated from the shift in Bragg wavelength ( $\Delta \lambda_B$ ), according to Equation 1:

$$\Delta n_{\text{eff}} = \Delta \lambda_B / 2\Lambda \quad (1)$$

where  $\Lambda$  is the period of the Bragg grating and is explicitly defined during the UV writing process. The change in birefringence of the Bragg grating ( $\Delta B_{\text{eff}}$ ) can be expressed as the difference in the shift in the effective index of the TE and TM modes as temperature or analyte are changed (Equation 2):

$$\Delta B_{\text{eff}} = \Delta n_{\text{eff}}^{\text{TE}} - \Delta n_{\text{eff}}^{\text{TM}} \quad (2)$$

$\Delta B_{\text{eff}}$ , is defined as zero at the initial conditions of analyte and temperature for the Bragg grating.

#### 4. Results and discussion

For the un-etched Bragg grating, the fundamental mode is largely symmetric. However, etching introduces strong birefringence,  $B$ , within the waveguide, greatly modifying the transverse magnetic (TM) and transverse electric (TE) mode profiles of the Bragg grating waveguide. It is found that the TE mode is much more sensitive to changes in the over-clad than the TM mode. Sputtering the sensor region with tantalum pentoxide (72.5 nm,  $n = 2.05$ ) pulls the evanescent field of the TE mode further out of the surface, not only increasing sensitivity but also further increasing the birefringence of the modes. This effect is illustrated in Figure 2, where the TM mode remains much more within the core of the waveguide. This increase in the birefringence of the two modes is sufficient to separate the two Bragg reflections to allow simultaneous acquisition. Figure 3 shows the response of the Bragg grating with a central wavelength of  $\sim 1540$  nm, to a series of Cargille refractive index liquids (Series AA and AAA) illustrating the increased sensitivity and birefringence of the two modes to changes in the analyte refractive index.

While the TE and TM modes have dramatically differing sensitivities to changes in the refractive index of the analyte, the TE and TM response to temperature fluctuations are much more closely matched. Dai *et al* [14] has shown that these properties can be used to decouple temperature fluctuations from changes in the analyte under interrogation. This method of temperature referencing allows for *in-situ* monitoring, an improvement over using a second Bragg grating as previously discussed.

However at the high sensitivities and broad range of analytes necessary for functional chemical sensors, these assumptions start to break down. This method [14] relies on two assumptions. Firstly that only one mode is sensitive to changes in the refractive index (i.e.  $d(n_{\text{eff}}^{\text{TM}})/dn \approx 0$ ) and secondly, that the thermal response for both modes are comparable ( $d(n_{\text{eff}}^{\text{TM}})/dT \approx d(n_{\text{eff}}^{\text{TE}})/dT$ ); combining these two assumptions into Equation 2, gives Equation 3.

$$\Delta B_{\text{eff}} = \Delta n_{\text{eff}}^{\text{TE}}(n, T) - \Delta n_{\text{eff}}^{\text{TM}}(n, T) \approx \Delta n_{\text{eff}}^{\text{TE}}(n) \quad (3)$$

This shows that the expression approximates to  $\Delta n_{\text{eff}}^{\text{TE}}(n)$ , i.e. the change in birefringence of the Bragg response is solely dependent on the TE response to analyte.

Figure 3 shows that for small changes in the analyte the assumption that TM is chemically insensitive holds up well. Even when changing between two pure solvents, such as water ( $n = 1.315$  at  $\lambda = 1550$  nm) and ethanol ( $n = 1.354$ ) [15], the shift in the peak Bragg wavelength of the TM mode is still small ( $\Delta n_{\text{eff}}^{\text{TM}} = 0.0003$ ), and is an order of magnitude smaller than that for TE ( $\Delta n_{\text{eff}}^{\text{TE}} = 0.0034$ ).

For the un-etched Bragg grating, the assumption that both fundamental modes have the same thermal response is reasonable (Figure 4(a)); both modes are exposed to similar silica environments and thus similar thermo-optic properties ( $dn/dT$ ). The thermo-optic constant can be measured for the buried Bragg grating to be  $10.49 \times 10^{-6} \text{ } ^\circ\text{C}^{-1}$  at a wavelength of 1550 nm, consistent with typical values for bulk silica [16]. Etching and sputtering the surface, as described previously, increases the birefringence of the modes, but at low analyte indices the assumption still holds true. In air, the low refractive index pushes the two modes back within the silica waveguide and underclad, which combined with the lack of a thermo-optic component for air, again results in similar thermal properties between the two modes.

While this assumption has been shown to hold well in air [14], for the solvents required for chemical and biosensors the system becomes more complicated. The higher index of common solvents pulls the evanescent field from the waveguide into the solvent. The Bragg grating no longer senses just the silica, but a mixture of the silica and the surrounding fluid, and hence their associated thermo-optic components. If the TE and TM mode were equally affected by the presence of the solvent, the gradient of Figure 4(a) would be altered to reflect the amalgamation of the various  $dn/dT$  values, but the modes would respond equally.

However, as shown in Figure 2, the penetration of the evanescent field into the analyte differs considerably for the two modes. The effect of this is that the  $dn_{\text{eff}}/dT$  of the TE mode is dominated more by the  $dn/dT$  of the analyte than that of the TM mode – which is still dominated by the intrinsic coefficient of the silica waveguide. This is demonstrated in Figure 4(b); where immersing the sensor in deionised water results in little change in the  $dn_{\text{eff}}/dT$  of the TM mode, which contrasts with the suppressed response observed for the TE mode. The suppression of the  $dn_{\text{eff}}/dT$  of the TE mode is a result of the negative  $dn/dT$  of water. This is further complicated by the temperature dependence of the thermo-optic coefficient of water increasing the degree of suppression with temperature. For real world applications a simple subtraction between the modes as previously proposed is not only insufficient, but would enhance the thermal component rather than negate it.

Although the two modes are different, an understanding of the system allows the temperature dependence to be compensated. For many sensing applications the solvent used is consistent or at least known in advance. For example, many bio-sensing devices are run in water or a saline solution. For the TM mode to be used for temperature referencing to produce temperature-insensitive Bragg grating sensors, a scaling factor is needed. Modelling the system for the desired analyte or solvent allows the thermal properties of the two modes to be calculated. In addition this model can be used to determine a scaling factor,  $K$ , between the modes. Equation 3 can simply be modified to incorporate  $K$ , to give Equation 4:

$$\Delta B_{\text{eff}} = \Delta n_{\text{eff}}^{\text{TE}}(n,T) - K \cdot \Delta n_{\text{eff}}^{\text{TM}}(n,T) \quad (4)$$

For most solvents this approach works well providing accurate thermal referencing. With a suitable database of  $dn/dT$  for commonly used solvents, at the interrogation wavelength, this method can be fully incorporated into the grating analysis software. Figure 5 shows the measured response of a Cargille refractive index liquid (Series AAA, “1.3000”) to changes in temperature and the fitted response of the model of the system from Figure 2. This model was verified against

the analyte data shown in Figure 3 and can be used to find the value of ( $K = -1.21$ ) to allow temperature referencing for this fluid.

To test this approach, the Bragg grating sensor was cooled from 40 to 22 °C with the same Cargille refractive index liquid on the sensor window while the temperature was monitored with a thermocouple. As shown in Figure 6, the TM mode and TE mode demonstrated very different behaviours during this cooling curve experiment; however applying the scaled TE-TM normalisation removed the thermal component, and in the absence of any refractive index changes in the analyte, gave the flat line (red dash). In contrast, applying the simple subtraction of the two modes without the scaling factor,  $K$ , was shown to increase the thermal component of the TE mode rather than remove it (red dots). It is shown that by monitoring the TM mode a temperature-insensitive Bragg grating sensor can be produced that can compensate for analytes with very different properties from those of the silica waveguide.

For more complex solvents, such as water, where the gradient,  $dn/dT$  is highly temperature dependent (Figure 7),  $K$  is no longer a constant but becomes a function of temperature,  $K(T)$ , giving the relation:

$$\Delta B_{\text{eff}} = \Delta n_{\text{eff}}^{\text{TE}}(n,T) - K(T) \cdot \Delta n_{\text{eff}}^{\text{TM}}(n,T) \quad (5)$$

This would imply that the temperature must be known in advance to be able to apply this approach. However, over small changes in temperature (i.e.  $<5$  °C)  $K$  can be approximated to a constant and only an initial estimate of the ambient temperature or a temperature range is needed to apply this method to remove thermal fluctuations from the system. An un-etched reference grating can be used to provide this initial information.

## 5. Conclusion

It has been previously shown that the birefringence of the mode in an evanescent sensor can be used to compensate for temperature fluctuations [14]. Here we have shown that the assumption that  $d(n_{\text{eff}}^{\text{TM}})/dT \approx d(n_{\text{eff}}^{\text{TE}})/dT$  is not well suited for a liquid environment. By using the TM mode to monitor temperature fluctuations and, in conjunction with the thermo-optic constants for the solvents of the system, a temperature-insensitive Bragg grating sensor can be fabricated. It has been shown that for a real system this approach can successfully remove the thermal component from the Bragg response while the simple approximation fails. Not only does this approach simplify the system, as no additional components are necessary (e.g. a second Bragg grating or thermocouple), but it makes use of the previously redundant TM mode of the Bragg response. The high resolution of this method of temperature compensation combined with the high sensitivity of a planar Bragg grating makes this system ideal for detection of the subtle changes in chemical and bio-sensing applications.

## References

1. R. G. Hunsperger, *Integrated Optics: Theory and Technology*, Springer, Berlin, 2002.
2. J. Homola, *Surface Plasmon Resonance Based Sensors*, Springer, Berlin, 2006.
3. G.R. Quigley, R.D. Harris, J.S. Wilkinson, *Appl. Optics*. 38 (1999) 6036-6039.
4. R. D. Palma, W. Laureyn, F. Frederix, K. Bonroy, J.-J. Pireaux, G. Borghs, G. Maes, *Langmuir*. 23 (2007) 443-451.
5. M. Olivero, M. Svalgaard. *Opt. Express*. 13 (2005) 8390-8399.

6. D. O. Kundys, J. C. Gates, S. Dasgupta, C. B. E. Gawith, P. G. R. Smith, *IEEE Photonic. Tech. L.* 21 (2009) 947-949.
7. G. D. Emmerson, S. P. Watts, C. B. E. Gawith, V. Albanis, M. Ibsen, R. B. Williams, P. G. R. Smith, *Electron. Lett.* 38 (2002) 1531-1532.
8. C. B. E. Gawith, G. D. Emmerson, S. G. McMeekin, J. R. Bonar, R. I. Laming, R. B. Williams, P. G. R. Smith, *Electron. Lett.* 39 (2003) 1050-1051.
9. I.J.G. Sparrow, G. D. Emmerson, C.B.E. Gawith, P.G.R. Smith, M. Kaczmarek, A. Dyadyusha, *Appl. Phys. B.* 81 (2005) 1-4.
10. R. M. Parker, J. C. Gates, M. C. Gossel, P. G. R. Smith, *Appl. Phys. Lett.* 95 (2009) 173306 (3 pages).
11. K. Schroeder, W. Ecke, R. Mueller, R. Willsch and A. Andreev, *Meas. Sci. Technol.* 12 (2001) 757-764.
12. D. A. Pereira, O Frazao, J. L. Santos, *Opt. Eng.* 43 (2004) 299-304.
13. I. J. G. Sparrow, *Development and applications of UV written waveguides*, PhD Thesis, 2005.
14. X. Dai, S. J. Mihailov, R. B. Walker, *Meas. Sci. Technol.* 19 (2008) 045302-045307.
15. R. C. Kamikawachi, I. Abe, A. S. Paterno, H. J. Kalinowski, M. Muller, J.L. Pinto, J.L. Fabris, *Opt. Commun.* 281 (2008) 621-625.
16. J. Lee, C. Hahn, B. Wang, K. Reichard, D. Ditto, D. Glista, Q. Wang, S. Yin, *Opt. Commun.* 258 (2006) 184-192.

## Biography

Richard M. Parker is a postgraduate student studying for a PhD in Supramolecular functionalised Bragg sensors collaborating between the ORC and the School of Chemistry at the University of Southampton. He graduated from the University of Southampton with a MChem in Chemistry in 2007.

James C. Gates is currently a Research Fellow at the ORC at the University of Southampton. He gained an MPhys degree from the University of Southampton in 1999, and completed his PhD at the ORC in 2003. His PhD thesis investigated the optical properties of various photonic devices at a nanometre scale using an interferometric near-field technique. He continued researching in the field of nanophotonics in the Physics department at the University of Southampton before returning to the ORC in 2006. He is currently developing planar integrated optical devices for a wide range of applications in telecommunications and detection.

Martin C. Gossel has been a Senior Lecturer in the School of Chemistry at the University of Southampton since 1991 and Organic Chemistry Tutor at Christ Church, University of Oxford since 1973. He graduated from King's College, University of London, with a BSc in 1970 and a PhD in Physical Organic Chemistry in 1974.. He has published over 90 journal papers together with books, reviews and patents. His research interests have focussed on conformational analysis of small organic molecules, molecular electronics, crystal engineering and applications of photoactive polymers and dendrimers within the fields of biology, optoelectronics and materials science.

Peter G.R. Smith is a Professor in the ORC and the Department of Electronics and Computer Science at the University of Southampton. He graduated from Oxford University with a BA in Physics in 1990 and D.Phil in Nonlinear Optics in 1993. After a year spent as a management consultant he joined the University of Southampton. Peter has worked on a number of areas in optics ranging from laser spectroscopy to polymer integrated-optics. He has published over 180 journal and

conference papers in the fields of periodically poled materials and UV written devices, including invited talks at national and international meetings.

## Figure captions

Fig. 1 A schematic of the Bragg grating sensor (a), showing the effect of a high index overlayer on the guided mode (b).

Fig. 2 The modelled TE mode is pulled up into the tantalum pentoxide overlayer, resulting in a greater modal overlap with the analyte, however the evanescent field of the TM mode penetrates less out of the surface, resulting in much lower sensitivity to surface changes.

Fig. 3 Experimental data showing that an overlayer of tantalum pentoxide pulls the TE mode (cross) of the Bragg grating further into the analyte, enhancing the sensitivity to changes in refractive index of the analyte. The TM mode is also shown (circles) with little sensitivity. Both modes are consistent with modelling of the system (lines).

Fig. 4(a) The thermal response of  $\Delta n_{\text{eff}}$  for TE (solid) and TM (dashed) modes within an un-etched Bragg grating.

Fig. 4(b) The thermal response of  $\Delta n_{\text{eff}}$  for TE (solid) and TM (dashed) modes with a Bragg grating exposed to water.

Fig. 5 The thermal response of  $\Delta n_{\text{eff}}$  for TE (solid line) and TM (dashed line) modes with a Bragg grating exposed to a Cargille refractive index liquid of index 1.296 at 1550 nm, compared to the modelled system (points).

Fig. 6(a) The cooling curve recorded by the thermocouple.

Fig. 6(b) Applying the scaling factor,  $K$  to the TM (dashed line) and subtracting from the TE mode (solid line) makes the Bragg response insensitive to temperature changes (red dash) Without scaling TM by  $K$ , the thermal response of the TE mode is increased (red dots).

Fig. 7 The thermal response of  $\Delta n_{\text{eff}}$  for TE (solid line) and TM (dashed line) modes with a Bragg grating exposed to water compared to the modelled system (points).

Figure 1  
[Click here to download high resolution image](#)

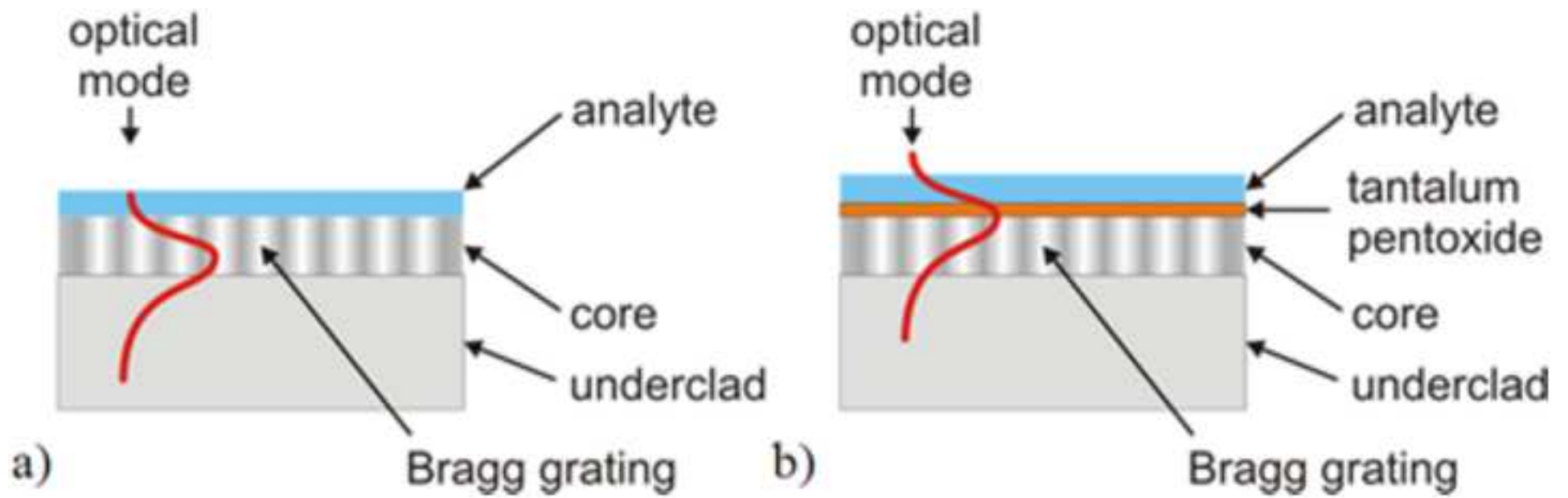


Figure 2  
[Click here to download high resolution image](#)

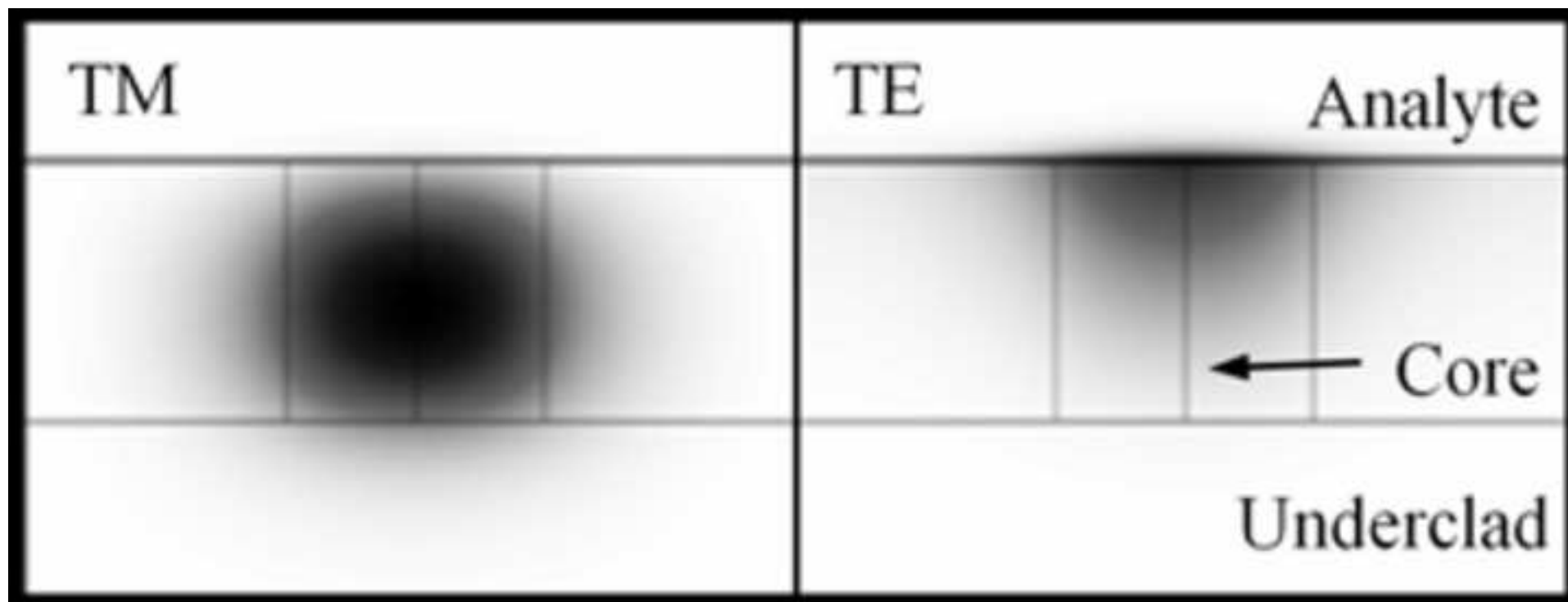


Figure 3  
[Click here to download high resolution image](#)

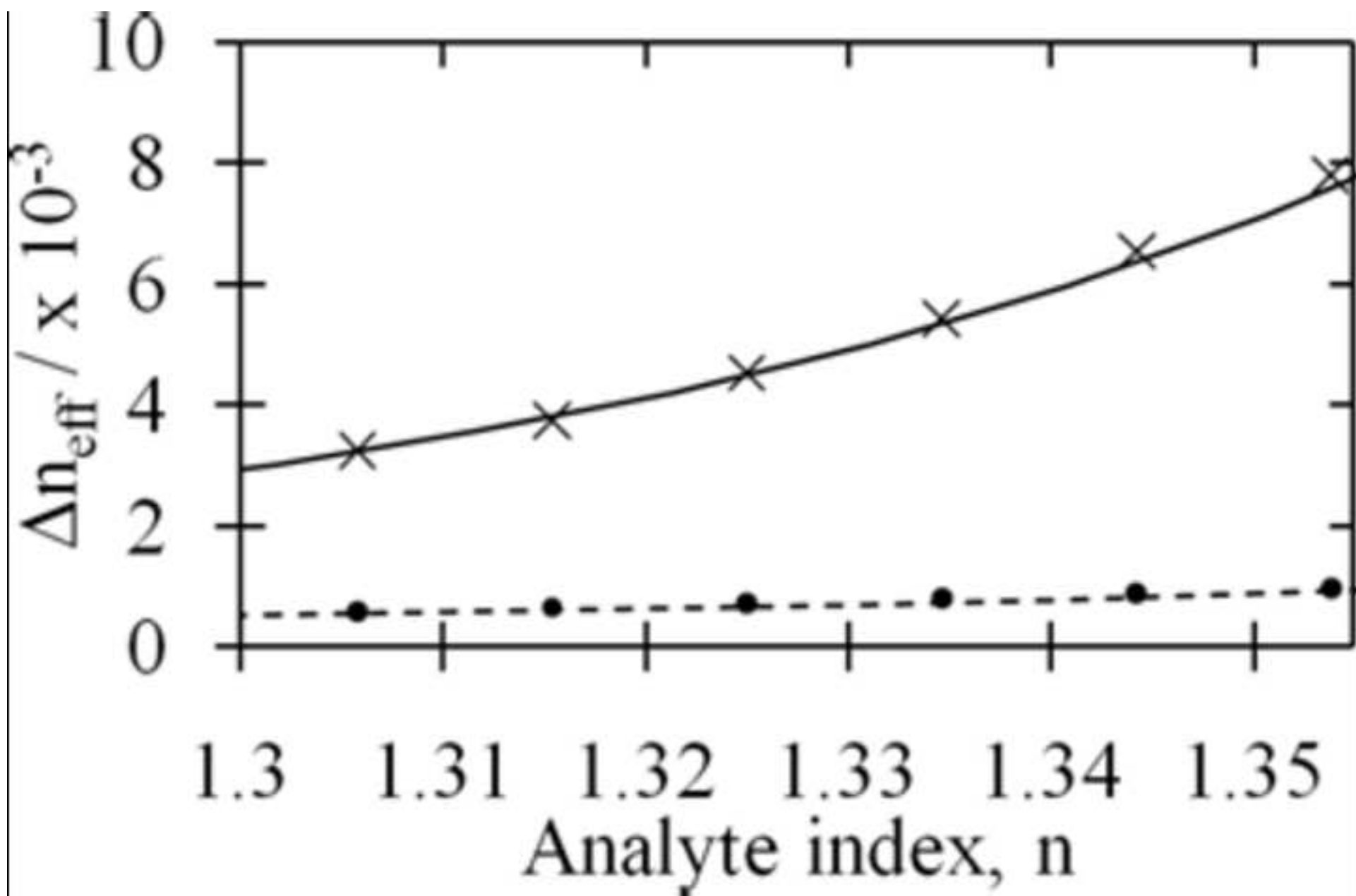


Figure 4  
[Click here to download high resolution image](#)

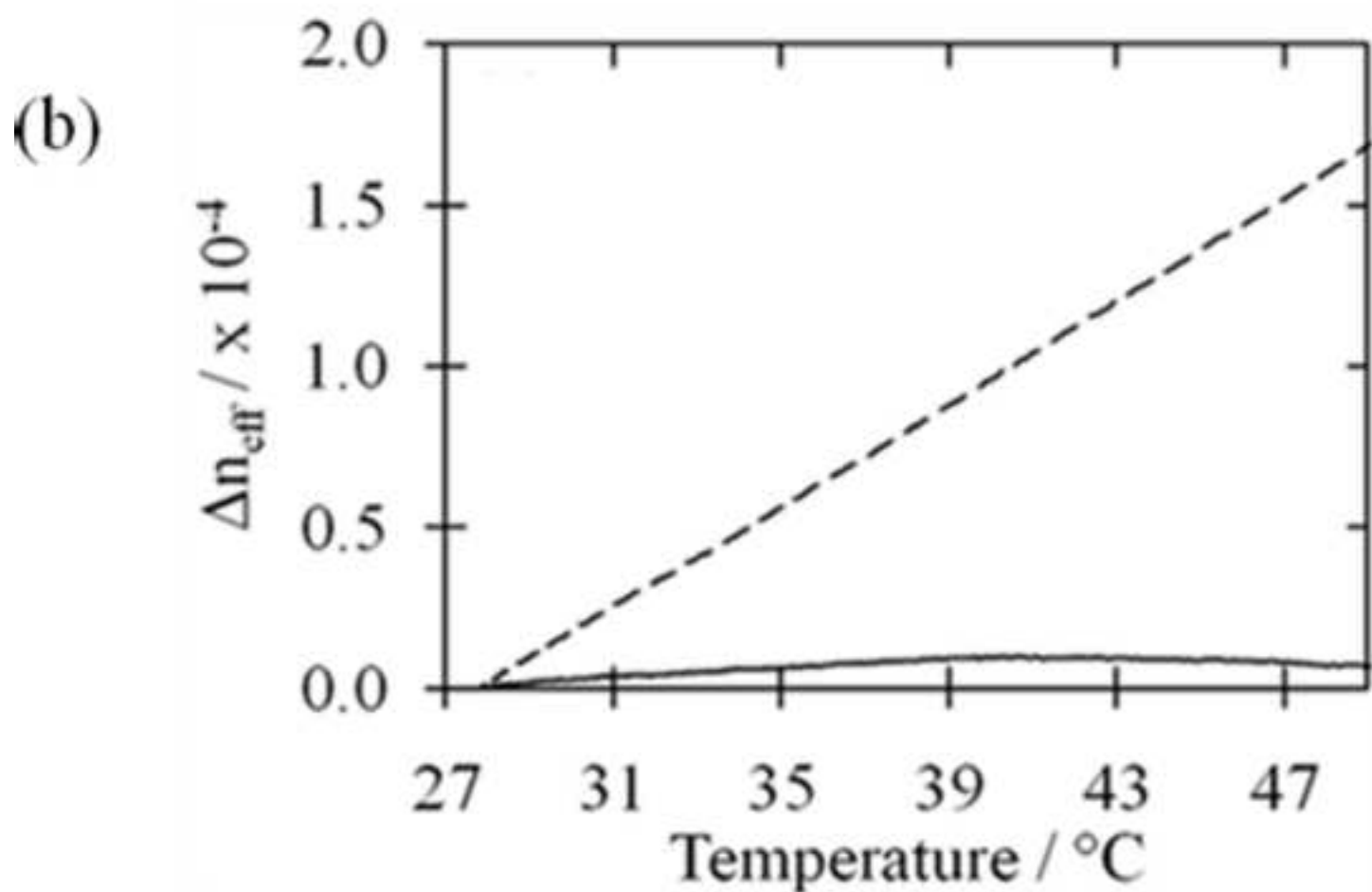
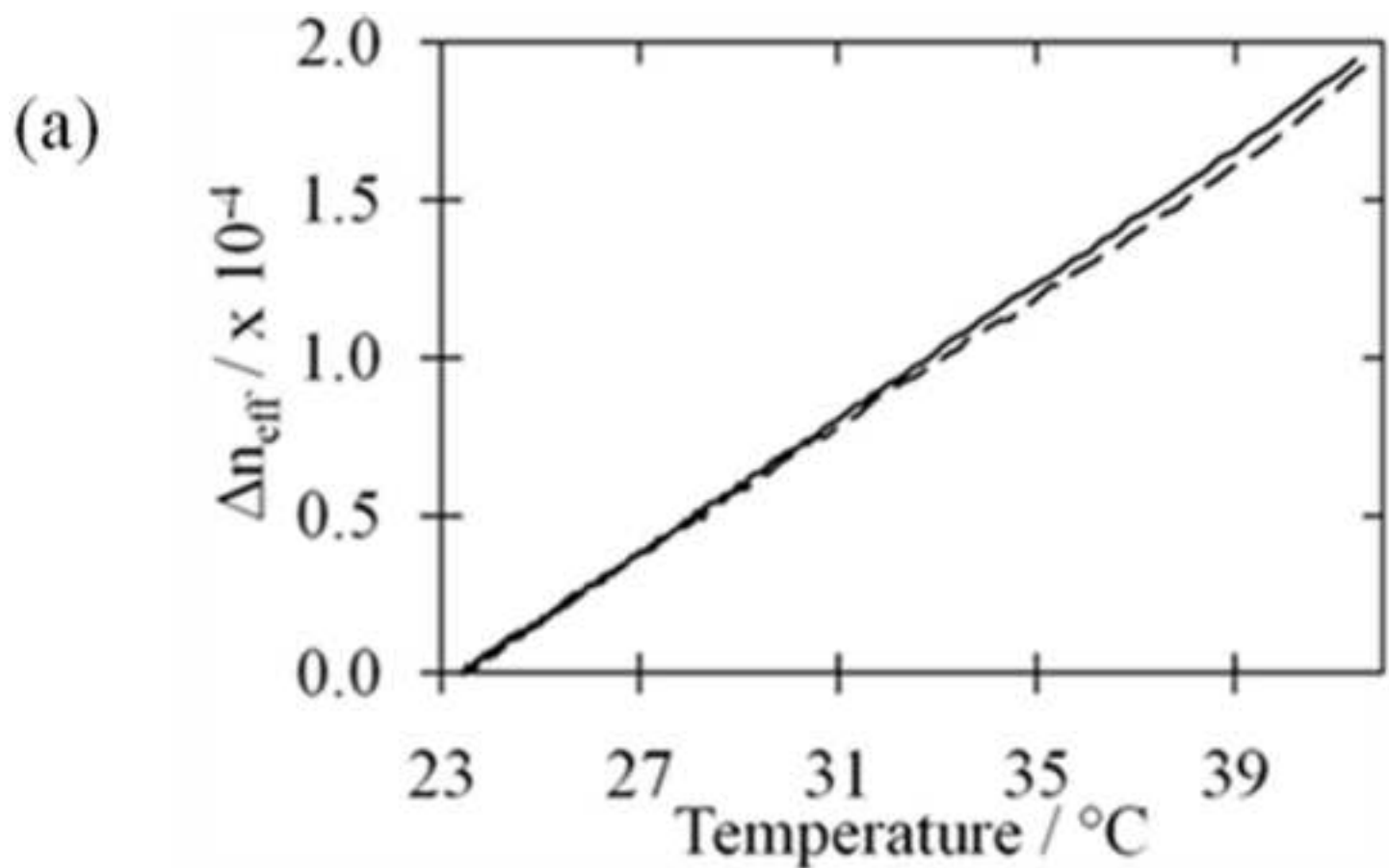


Figure 5  
[Click here to download high resolution image](#)

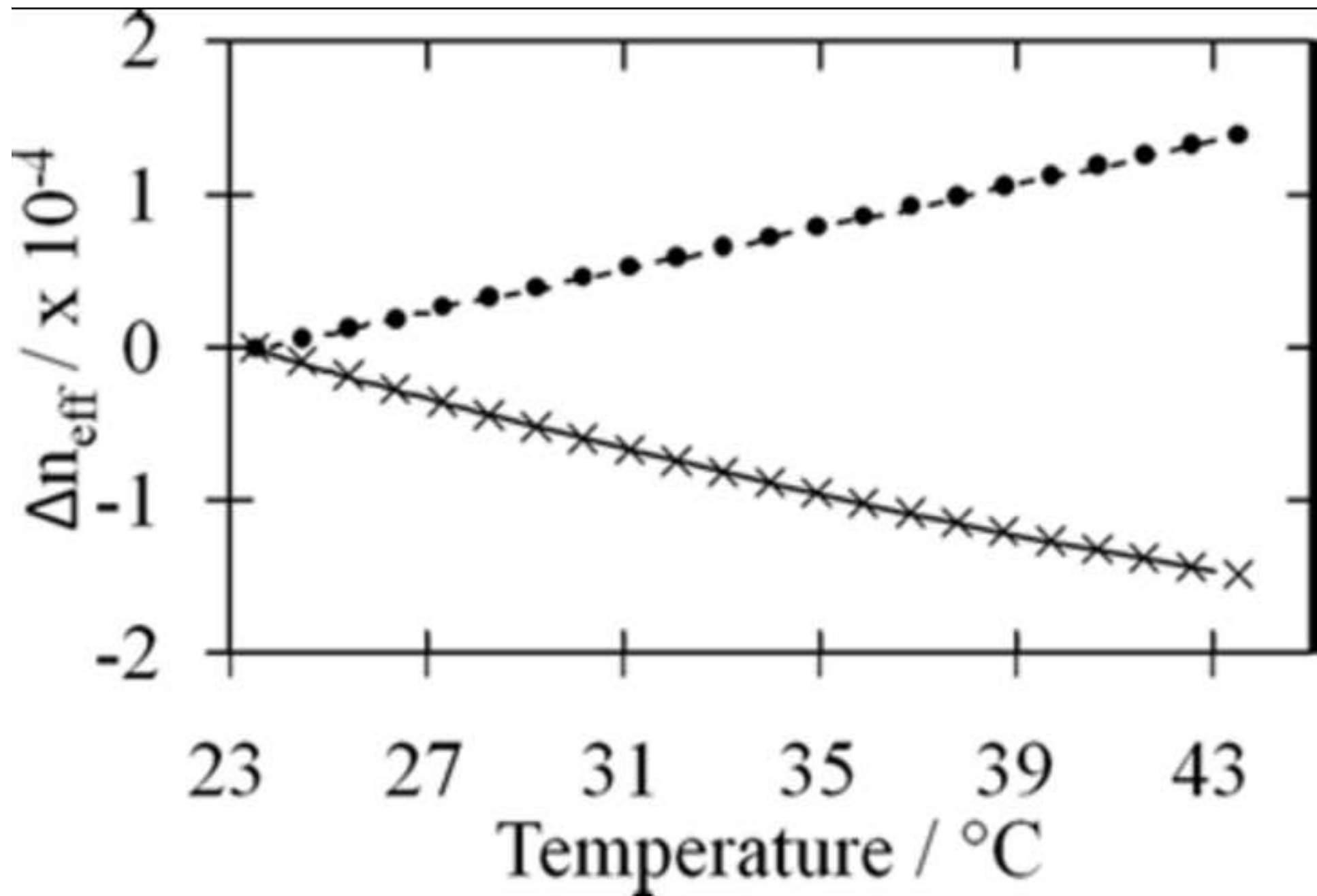


Figure 6  
[Click here to download high resolution image](#)

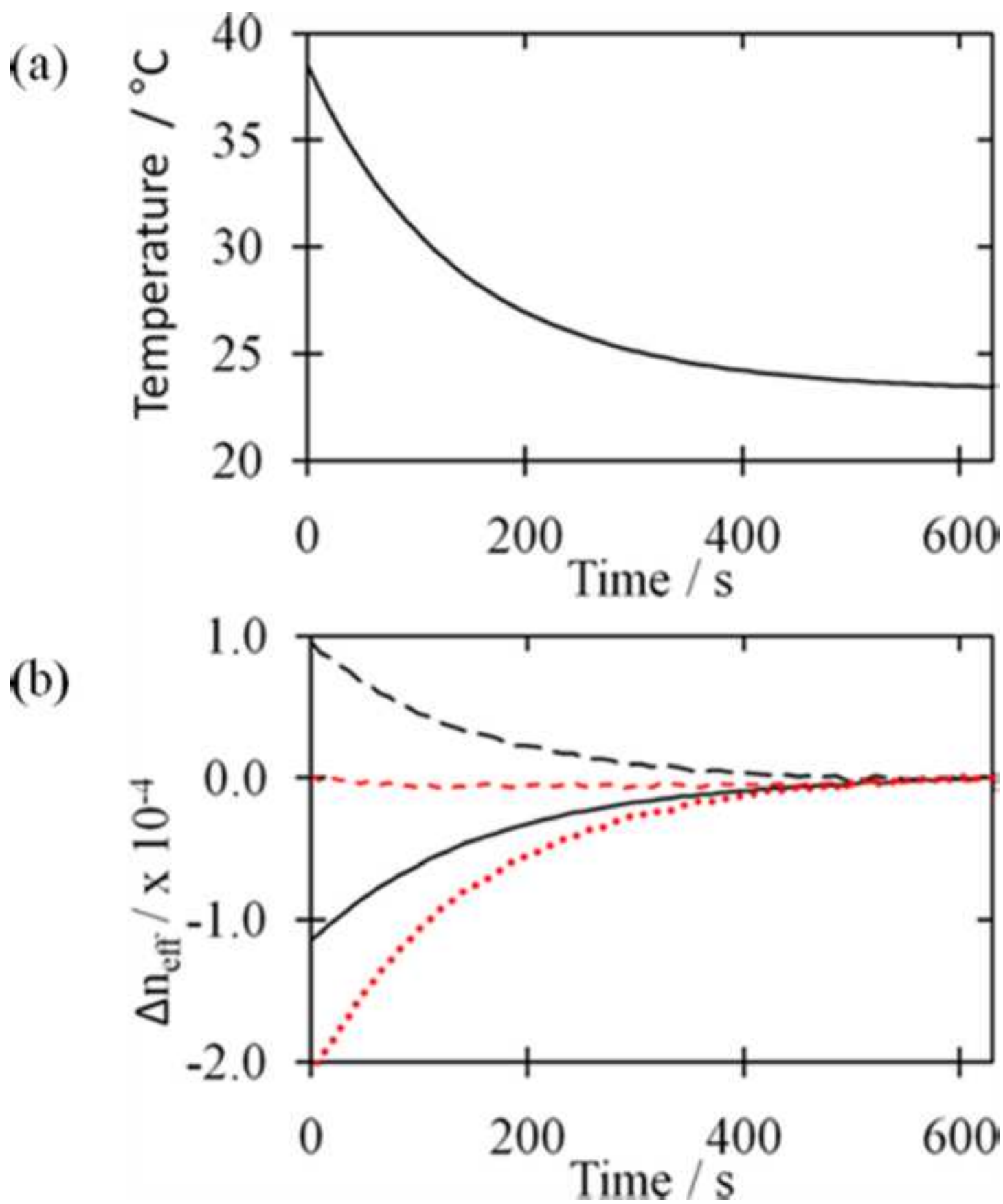


Figure 7  
[Click here to download high resolution image](#)

